Robust Observer-Based Dynamic Sliding Mode Controller for a Quadrotor UAV

NURADEEN FETHALLA[1], **MAAROUF SAAD**[1], **HANNAH MICHALSKA**[2], **AND JAWHAR GHOMMAM**[3]

[1]Electrical Engineering Department, École de technologie supérieure, Montreal, QC H3C 1K5, Canada
[2]Electrical and Computer Engineering Department, McGill University, Montreal, QC H3A 0G4, Canada
[3]Department of Electrical and Computer Engineering, Sultan Quaboos University, Muscat 123, Oman

Corresponding author: Nuradeen Fethalla (nuradeen.fethalla.1@ens.etsmtl.ca)

ABSTRACT In this paper, a novel robust backstepping-based approach combined with sliding mode control is proposed for trajectory tracking of a quadrotor UAV subject to external disturbances and parameter uncertainties associated with the presence of aerodynamic forces and possible wind force. To enhance robustness, a nonlinear disturbance observer (NDO) is employed alongside the controller. A sliding surface is introduced, which shares intermediate control goals with a conventional backstepping scheme. The closed-loop system comprising the sliding mode and backstepping controllers is finally combined with the NDO to track the desired position and attitude trajectories. Good tracking is achieved in the closed loop if the controller and observer gains are selected correctly. The system performance exhibits much better robustness than the existing backstepping control methods, which are not equipped with nonlinear disturbance estimators. The simulation results are confirmed in terms of real laboratory experiments. Prior to the implementation of the control method, the real system has been identified and calibrated.

INDEX TERMS Quadrotor UAV, backstepping control, sliding mode control, nonlinear disturbance observer (NDO).

I. INTRODUCTION

Quadrotor UAVs have many important applications. It is hence not surprising that the control problem for quadrotors and other rotorcraft has recently received much attention. A vast literature exists on this topic in which both linear and nonlinear control schemes have been proposed for the attitude and position control of the quadrotor. Proportional-Integral-Derivative (PID) attitude control and Linear Quadratic Regulator (LQR) attitude control were studied in [6]. Robustness properties of the conventional SMC are, however, limited to matched disturbances and uncertainties; see [17] for the definition of matched disturbances. Unfortunately, there are many important nonlinear system applications in which the matched disturbance property is invalid [19]. The quadrotor UAV systems in [7] and [18] are leading examples of nonlinear systems that belong to this category. For this reason alone, most of the existing sliding mode controllers for quadrotor UAVs predominantly attenuate the uncertainties that are matched to the control input, i.e. uncertainties that can be instantaneously and directly compensated for by the system input [20], [21].

The disturbance matching condition is restrictive and is not met in many practical UAV systems. In the case of a quadrotor UAV system, the uncertainties comprise perturbations of model parameters which are combined with the unknown aerodynamic forces and also possibly the external effects due to atmospheric winds. The latter act on the UAV system via different channels (enter different state equations of the system). Many of such disturbances affect state equations with no direct dependence on the control input [24]. In this situation, the application of a conventional sliding mode control (SMC) leads to severe limitations in achieving asymptotic set point control; the closed loop system can only be stabilized to a neighborhood of a stationary point whose size is commensurate with the magnitude of the unmatched disturbance [19].

Many authors have hence made efforts of designing sliding surfaces with improved robustness properties [22], [23]. Classical backstepping and conventional sliding mode control designs presented in [7] and [8] offer a robust backstepping control approach based on the concept of the Direction Cosine Matrix (DCM). The DCM method shown satisfactory

robustness properties. A backstepping controller for complete stabilization of a quadrotor UAV was proposed in [9]. However, the majority of existing control designs are still not sufficiently robust with respect to unknown dynamics or system perturbations which adversely affects flight control performance.

In many quadrotor models available in the literature, it is assumed that the hover speed of the quadrotor during its mission is low, so the influence of the external aerodynamic forces and the torque disturbances can simply be neglected. However, in realistic flight conditions, the nonlinear aerodynamic forces, the wind gusts, and torque disturbances can be powerful enough to destabilize the vehicle or knock it off the desired trajectory, [10]. Although the backstepping control approach, [12], is a powerful technique to deal with system nonlinearities, it applies to models of somewhat restricted structure. Moreover, the complexity of conventional backstepping control increases disproportionally with the dimension of the system to be steered. In this regard, robust versions of the backstepping are much better but need full state measurement [11]. To simplify the implementation of robust backstepping, direct on-line differentiation of the measured output was proposed to recover the full state of the system, [14]. A command filter was introduced in [15] to obviate the need to compute analytic derivatives and to create virtual signals to increase the degree of robustness of the backstepping controller.

Further attempts to increase the robustness of the quadrotor control schemes include a high order sliding mode controller developed in [13] that is able to reject the influence of some of the uncertainties in the system. The robust controller of [13] also attenuates chattering of the traditional sliding mode control approach.

The NDO-SMC control is already widely used in robotics where it can achieve diverse objectives. [25]. The SMC methods attempt to compensate for the unmatched uncertainties by utilizing bounds on the disturbances along with bounds on their first derivatives. The most restrictive requirement encountered in many nonlinear disturbance observers is that the time derivatives of the disturbances need to approach zero.

In this context, the consensus is that the best control approaches employ nonlinear disturbance observers in conjunction with nonlinear control. In our previous work, [1], [2], the proposed UAV control approach employed an NDO in conjunction with two separated control blocks: using backstepping and SMC. In contrast, the approach presented here fully combines the actions performed by the NDO, backstepping, and SMC. Additionally, numerical simulation results are confirmed here by experimental results performed under laboratory conditions.

Recognizing the importance of robustness in practical control of UAVs, a novel observer-based feedback control design is proposed that comprises three concepts: (1) nonlinear sliding mode control, (2) robust backstepping as assisted by (3) a nonlinear disturbance observer. The systematic design procedure carefully combines the interacting translational

and rotational control subsystems by the use of intermediate fictitious control variables. The task of the backstepping controller is predominantly to stabilize the translational subsystem while the SMC simultaneously steers the rotational subsystem. The NDO provides the estimates of all the disturbances both matched and unmatched insuring very good robustness of the combined feedback controls.

The novel contributions are hence summarized as follows:
 (i) The proposed approach yields the first combined SMC and backstepping controller that employs an NDO to compensate for all disturbances and model-system error. Although the same type of NDO was also used in [16], its convergence properties were not assessed fully.
(ii) In comparison with [13], our results show that the robustness of the closed-loop control system is increased by the presence of the NDO.
(iv) Laboratory experiments were preceded by proper identification and calibration of the real system;
 (v) The laboratory experiments reproduced the simulation results with high fidelity despite using a fan to simulate wind gusts.

The paper is organized as follows: the dynamic model of a quadrotor UAV is presented in section II. The problem formulation and control objectives are stated in section III. The design of the NDO and the associated backstepping-sliding mode controller for position and attitude subsystems are described in sections IV-A, IV-B, and IV-C respectively. Section V delivers the stability analysis of the closed loop system. Model parameter identification of the real quadrotor is described in section VI. The performance of the proposed approach is assessed in simulations in section VII as well as in the experimental laboratory setting in section VIII followed by the conclusions in section IX.

II. DYNAMIC MODELING OF A QUADROTOR
The dynamic model of the considered quadrotor UAV, shown in Fig.1, is originally described in [3] and again employed in [4] and [5].
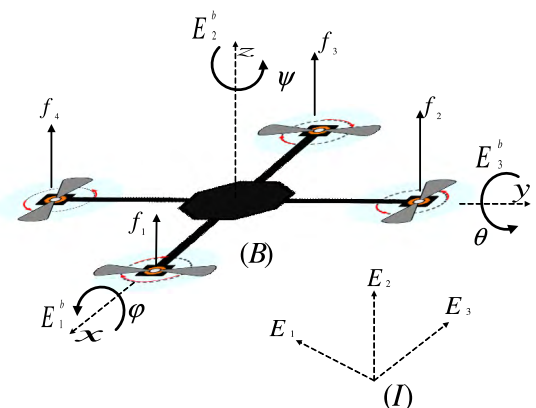

FIGURE 1. Quadrotor airframe and reference frames configuration.

Let us consider two main reference frames: the earth fixed frame ($\mathcal{I}$) associated with the unit vector basis (E_1, E_2, E_3)

and body fixed frame ($\mathcal{B}$) associated with the unit vector basis (E_1^b, E_2^b, E_3^b) fixed at the center of mass of the quadrotor, as shown in Fig.1. The position of the center of the quadrotor's mass is denoted by the vector $p = [x, y, z]^T$. This position vector is expressed with respect to an inertial frame ($\mathcal{I}$). The attitude is denoted by $\Theta = [\psi, \theta, \phi]$. These three angles are the Euler angles yaw ($-\pi < \psi < \pi$), pitch ($-\frac{\pi}{2} < \theta < \frac{\pi}{2}$), and roll ($-\frac{\pi}{2} < \phi < \frac{\pi}{2}$) that define the orientation vector of the quadrotor with respect to the inertial frame ($\mathcal{I}$). Define the angular velocity and acceleration of roll, pitch, and yaw as $\Omega = [\Omega_p, \Omega_q, \Omega_r]^T$ with respect to the body-fixed frame ($\mathcal{B}$), and $\ddot{\Theta} = [\ddot{\phi}, \ddot{\theta}, \ddot{\psi}]$ with respect to the inertia reference frame $\mathcal{I}$. The linear velocities and accelerations of the translational system are given respectively as $\dot{p} = [\dot{x}, \dot{y}, \dot{z}]$, and $\ddot{p} = [\ddot{x}, \ddot{y}, \ddot{z}]$. The transformation between the body-fixed reference frame $\mathcal{B}$ and the inertial reference frame $\mathcal{I}$ in the space orientation of the quadrotor is given by the rotation matrix R and Euler matrix $M(\Theta)$. These matrices are given by

$$R(\Theta) = \begin{bmatrix} C_\theta C_\psi & S_\phi S_\theta C_\psi - C_\phi S_\psi & C_\phi S_\theta C_\psi + S_\phi S_\psi \\ C_\theta S_\psi & S_\phi S_\theta S_\psi + C_\phi C_\psi & C_\phi S_\theta S_\psi - S_\phi c_\psi \\ -S_\theta & S_\phi C_\theta & C_\phi C_\theta \end{bmatrix}$$

$$M(\Theta = \begin{bmatrix} 1 & 0 & -S_\theta \\ 0 & C_\phi & S_\phi C_\theta \\ 0 & -S_\phi & C_\phi S_\theta \end{bmatrix}$$

where the relationship between $\dot{\Theta}$ and Ω can be described as

$$\Omega = M(\Theta)\dot{\Theta} \qquad (1)$$

An extended formulation of these transformations can be found in [5].

The quadrotor dynamic equations will be written in the form of two subsystems corresponding to translational motion (referring to the position of the center of mass of the UAV) and angular motion (referring to the attitude of the UAV). These equations can be stated in the reference frame ($\mathcal{I}$) as

$$\ddot{p} = \frac{1}{m}R(\Theta)F_{prop} - G + d_p(t)$$
$$\ddot{\Theta} = (IM(\Theta))^{-1}[T_{prop} - IN(\Theta, \dot{\Theta}) \qquad (2a)$$
$$\qquad - \Omega \times I\Omega - T_g] + d_\Theta(t)$$
$$\qquad = \Phi(\Theta, \dot{\Theta}) + \Psi(\Theta)T_{prop} + d_\Theta(t) \qquad (2b)$$

where $N(\Theta, \dot{\Theta})$ is given by

$$N(\Theta, \dot{\Theta}) = \begin{bmatrix} -C_\theta \dot{\theta}\dot{\psi} \\ -S_\phi \dot{\phi}\dot{\theta} + C_\phi \dot{\phi}\dot{\psi} - S_\phi S_\theta \dot{\theta}\dot{\psi} \\ -C_\phi \dot{\phi}\dot{\theta} - S_\phi C_\theta \dot{\phi}\dot{\psi} - C_\phi S_\theta \end{bmatrix}$$

and T_d is the resultant torques due to the gyroscopic effects given as

$$T_d = \sum_{i=1}^{4} \Omega \times J_r[0, 0, (-1)^{i+1}\omega_i]^T \qquad (3)$$

where J_r is the moment of inertia of each rotor and ω_i, $i = 1, 2, 3, 4$ is the rotary speed of each motor. $\Psi(\Theta)$ and $\Phi(\Theta, \dot{\Theta})$ are defined as

$$\Psi(\Theta) = (IM(\Theta))^{-1}$$
$$\Phi(\Theta, \dot{\Theta}) = -(IM(\Theta))^{-1}[IN(\Theta, \dot{\Theta}) - \Omega \times I\Omega - T_g]$$

The matrix $I = diag(I_x, I_y, I_z)$ is the inertia matrix of the quadrotor; $G = [0, 0, -g]^T m/s^2$ is the gravitational force acting in the z-direction; m denotes the mass of the quadrotor. The terms $d_p = [d_x \ d_y \ d_z]^T$ and $d_\Theta = [d_\phi \ d_\theta \ d_\psi]^T$ model smooth and bounded external disturbances along with the aerodynamical disturbances. The functions $S_{(\cdot)}$ and $C_{(\cdot)}$ denote $\sin(\cdot)$ and $\cos(\cdot)$, respectively. Assuming that each motor produces thrust and drag that are proportional to the square of the motor speed, the force generated by the ith motor is given by $f_i = b\omega_i^2(i = 1, 2, 3, 4)$ where b is the thrust factor. F_{prop} and T_{prop} are: the three-dimensional translational force vector and the three-dimensional reaction moment vector exerted by the propellers, respectively, as given by

$$F_{prop} = \begin{bmatrix} 0 \\ 0 \\ T \end{bmatrix} \qquad T_{prop} = \begin{bmatrix} h(f_4 - f_2) \\ h(f_3 - f_1) \\ c\sum_{i=1}^{4}(-1)^i f_i \end{bmatrix}$$

where $T = \sum_{i=1}^{4} f_i$ is the total thrust, h is distance from the center of mass to the rotor, and c is he drag factor coefficient. It is easy to verify that equations (2a)-(2b) can actually be written as

$$\ddot{\phi} = r_1\dot{\theta}\dot{\psi} - r_2\dot{\theta}w + q_1U_2 + d_\phi$$
$$\ddot{\theta} = r_3\dot{\phi}\dot{\psi} + r_4\dot{\phi}w + q_2U_3 + d_\theta$$
$$\ddot{\psi} = r_5\dot{\theta}\dot{\phi} + q_3U_4 + d_\psi$$
$$\ddot{x} = (C_\phi S_\theta C_\psi + S_\phi S_\psi)\frac{1}{m}U_1 + d_x$$
$$\ddot{y} = (C_\phi S_\theta S_\psi - S_\phi C_\psi)\frac{1}{m}U_1 + d_y$$
$$\ddot{z} = -g + (C_\phi C_\theta)\frac{1}{m}U_1 + d_z \qquad (4)$$

where $[U_1, U_2, U_3, U_4]^T = [T, T_{prop}]^T$ is the input vector.

$$r_1 = \frac{I_y - I_z}{I_x}, \quad r_2 = -\frac{J_r}{I_x}, \quad r_3 = \frac{I_z - I_x}{I_y}, \quad r_4 = \frac{J_r}{I_y},$$
$$r_5 = \frac{I_x - I_y}{I_z}, \quad q_1 = \frac{h}{I_x}, \quad q_2 = \frac{h}{I_y}, \quad q_3 = \frac{1}{I_z}$$

are inertia related constants and $\omega = \omega_4 + \omega_3 - \omega_2 - \omega_1$. The state vector X can thus be defined as

$$X = [p \ \dot{p} \ \Theta \ \dot{\Theta}]^T \in \mathbb{R}^{12}$$

III. PROBLEM FORMULATION

The dynamic model (4) of the quadrotor UAV is now conveniently viewed as a system composed of two subsystems, the position subsystem and the rotational subsystem. It can be noted that the disturbances d_Θ and d_z are matched while the rest of the disturbances d_x and d_y are unmatched. The idea is to apply a nonlinear disturbance observer to each

subsystem separately, to remove the influence of matched and unmatched disturbances from the state variables in those subsystems. Considering (4), the objective is to design a controller that makes the state variables $[p, \psi]$ attain and follow their desired reference counterparts $[p_d, \psi_d]$. We make the following assumptions about the matched as well as the unmatched disturbances in the model (4).

Assumption 1: For each subsystem, it is assumed that, the matched and unmatched perturbations are differentiable with bounded derivatives, i.e.

$$\|\dot{d}_p(t)\| \leqslant D_p, \quad |\dot{d}_\Theta(t)| \leqslant D_\Theta \ t > 0 \tag{5}$$

for some positive constants D_p, D_Θ.

IV. THE COMBINED NDO-BASED BACKSTEPPING AND SLIDING MODE CONTROL

A. NONLINEAR DISTURBANCE OBSERVER DESIGN

In terms of flight performance, uncertainties cannot be neglected. To improve the robustness and stability of the overall control system an NDO is employed to estimate the matched and unmatched external disturbances in the quadrotor system. The NDO is introduced by Yang *et al.*. [16] and can be employed in a similar form for both subsystems (position and orientation):

$$
\begin{aligned}
\dot{z}_p &= -L_p z_p - L_p[L_p \dot{p} + G + \frac{1}{m} U_p] \\
\hat{d}_p &= z_p + L_p \dot{p} \\
\dot{z}_\Theta &= -L_\Theta z_\Theta - L_\Theta[L_\Theta \dot{\Theta} + \Phi(\Theta, \dot{\Theta}) - U_\Theta] \\
\hat{d}_\Theta &= z_\Theta + L_\Theta \dot{\Theta}
\end{aligned}
\tag{6a}
\tag{6b}
$$

where $U_p = R(\Theta)E_3 U_1$, $U_\Theta = \Psi(\Theta)[U_2 \ U_3 \ U_4]^T$, and $\hat{d}_j$ $(j = p, \Theta)$ is the estimation of the disturbance. The variable z_j is the state vector of the observer, and $L_j = L_j I_{3\times3}$, $L_j > 0$, $j = p, \Theta$, are the observer gain matrices to be tuned.

The following lemma will be helpful in proving convergence of the observer as well as the control scheme.

Lemma 1: Let $\dot{x} = f(x)$ be a smooth multivariate dynamic system with $x \in \mathbb{R}^n$, with $f(0) = 0$. Let V be a Lyapunov function that is strictly positive definite, continuously differentiable, radially unbounded, with $V(0) = 0$. Let $\mathcal{C} \subset \mathbb{R}^n$ be any given connected, compact set of initial conditions for the dynamic system. Finally, assume that along any trajectory of the system, $x : \mathbb{R}^+ \to \mathbb{R}^n$, starting in $\mathcal{C}$, the following differential inequality

$$\frac{d}{dt}\{V(x(t))\} < -\alpha V(x(t)) + \beta \quad \text{for all } t \geq 0$$
$$\text{with } x(0) \in \mathcal{C} \tag{7}$$

is satisfied with $\beta > 0$ as a fixed positive constant and α as a positive parameter that can be tuned. Under these conditions: for every $\epsilon > 0$ there exist an $\alpha^* > 0$ such that for all $\alpha \geq \alpha^*$ all trajectories of the dynamic system starting in $\mathcal{C}$ are bounded by the selected value of ϵ, i.e.

$$||x(t)||^2 \leq \epsilon, \quad \text{for all } t > T^*, \tag{8}$$

for a sufficiently large time T^*.

Proof: It is first convenient to define a function which is the composition of the Lyapunov function $V : \mathbb{R}^n \to \mathbb{R}^+$ with any given and admissible system trajectory function $x : \mathbb{R} \to \mathbb{R}^n$, $x(0) \in \mathcal{C}$, i.e. a function $W : \mathbb{R}^+ \to \mathbb{R}^+$ such that

$$W(t) := V(x(t)); \quad t \geq 0 \tag{9}$$

It is obvious that inequality (7) re-writes as

$$\frac{d}{dt}W(t) < -\alpha W(t) + \beta \quad \text{for all } t \geq 0 \tag{10}$$
$$\text{for any } W(0) := W_0 = V(x_0) \in V(\mathcal{C}) \tag{11}$$

where the image set $V(\mathcal{C})$ is compact as V is continuous hence maps compact sets into compact sets; in fact it is a compact interval in $\mathbb{R}^+$. The dependence of W on x is suppressed here as, by assumption, inequality (10) holds for any trajectory x of system $\dot{x} = f(x)$ passing through any initial condition $x(0) := x_0 \in \mathcal{C}$.

Consider an equation for a different function $W^* : \mathbb{R}^+ \to \mathbb{R}^+$, given by

$$\frac{d}{dt}W^*(t) = -\alpha W^*(t) + \beta; \tag{12}$$

with the same parameters $\alpha > 0$, $\beta > 0$, but with an initial condition $W^*(0) := W_0^* \notin V(\mathcal{C})$ that satisfies

$$W_0^* > w \quad \text{for all } w \in V(\mathcal{C}) \tag{13}$$

Its unique solution valid for all $t \geq 0$ is

$$W^*(t) = W_0^* \exp\{-\alpha t\} + \frac{\beta}{\alpha}[1 - \exp\{-\alpha t\}]$$
$$\text{so } W^*(t) \to \frac{\beta}{\alpha} \text{ as } t \to \infty \tag{14}$$

We shall now show that any system trajectory, $x(t); t \geq 0$, that implicitly satisfies (10) - (11) is majorized by the trajectory $W^*(t); t \geq 0$, i.e.

$$W(t) < W^*(t); \quad t \geq 0 \tag{15}$$

Clearly, $W(0) < W^*(0)$ by virtue of (13). The demonstration of (15) will be conducted by contradiction. To this end, if (15) were false then there would exist an initial condition $W_0 \in V(\mathcal{C})$ and a corresponding trajectory $W(t); t \geq 0$, for which the following set is nonempty:

$$Z := \{t \geq 0 \mid W(t) \geq W^*(t)\} \tag{16}$$

Defining $t_1 := \inf Z$, it is clear from (13) that $t_1 > 0$. Also

$$W(t_1) = W^*(t_1) \tag{17}$$

and

$$W(t) < W^*(t) \quad \text{for } t \in [0, t_1) \tag{18}$$

By virtue of the above (17) - (18), for sufficiently small, but negative $h < 0$ the following inequality holds

$$\frac{W(t_1+h)-W(t_1)}{h} > \frac{W^*(t_1+h)-W^*(t_1)}{h} \tag{19}$$

which, in the limit as $h \to 0$, implies that

$$\frac{d}{dt} W(t_1) \geq \frac{d}{dt} W^*(t_1) \qquad (20)$$

The assumption of the Lemma expressed in the form of (10) together with above (20) and (12) and (17) imply that there exists a trajectory $x(t)$; $t \geq 0$, with $x(0) \in \mathcal{C}$ such that, at some instant $t_1 > 0$:

$$-\alpha W(t_1) + \beta > \frac{d}{dt} W(t_1)$$
$$\geq \frac{d}{dt} W^*(t_1) = -\alpha W^*(t_1) + \beta$$
$$\text{so} \ \ W(t_1) < W^*(t_1) \ \text{since} \ -\alpha < 0. \qquad (21)$$

Inequality (21) is a clear contradiction of (17). So, Z is empty for all trajectories $W(t)$; $t \geq 0$, starting in $V(\mathcal{C})$. Hence (15) holds true, as claimed.

It then follows that all system trajectories that satisfy (10) - (11) are majorized by (14); i.e.

$$W(t) < W_0^* \exp\{-\alpha t\} + \frac{\beta}{\alpha}[1 - \exp\{-\alpha t\}]; \quad t \geq 0 \qquad (22)$$

Now, it is easy to see that for any W_0^* satisfying (13)

$$W_0^* \exp\{-\alpha t\} \leq \frac{\beta}{\alpha} \quad \text{for all} \ t \geq T(\alpha) \qquad (23)$$

with

$$T(\alpha) := \frac{1}{\alpha} \ln \left(\frac{W_0^* \alpha}{\beta} \right) \qquad (24)$$

Combining (22) with (23) gives

$$W(t) < 2\frac{\beta}{\alpha} \quad \text{for all} \ t \geq T(\alpha) \qquad (25)$$

along any trajectory of the system $x(t)$; $t \geq 0$, with $x(0) \in \mathcal{C}$, because the second term of (22) never exceeds β/α. Selecting an arbitrary positive constant $R > 0$, while setting

$$\alpha^* := \frac{2\beta}{R}; \quad T^* := T(\alpha^*) \qquad (26)$$

gives

$$W(t) < 2\frac{\beta}{\alpha} \leq R \quad \text{for all} \ t \geq T^*, \alpha \geq \alpha^* \qquad (27)$$

Denote a sublevel set of V by

$$V_R := \{x \mid V(x) \leq R\} \qquad (28)$$

Since the Lyapunov function V is continuous and radially unbounded its sublevel sets are bounded so there exists a ball $B(0; \sqrt{(\epsilon)})$ which contains the sublevel set V_R. By virtue of (27) it follows that if $\alpha \geq \alpha^*$ then for all times $t \geq T^*$ any system trajectory starting from the set $\mathcal{C}$ satisfies $W(t) = V(x(t)) \leq R$. This is to say that all such $x(t)$; $t \geq T^*$, remain in the sublevel set V_R, i.e. $x(t) \in V_R \subset B(0; \sqrt{(\epsilon)})$, which immediately implies that

$$||x(t)||^2 \leq \epsilon \quad \text{for all} \ t \geq T^* \qquad (29)$$

as required. ∎

Remark 1: It should be noted that the assumption of Lemma 1 is stated as a sharp differential inequality entirely for the simplicity of the proof and thus can be replaced by a non-sharp inequality as long as $\beta > 0$ because any slightly tighter non-sharp inequality such as

$$\frac{d}{dt}\{V(x(t))\} \leq -\alpha V(x(t)) + \frac{1}{2}\beta \quad \text{for all} \ t \geq 0 \qquad (30)$$

clearly implies a sharp inequality (7).

We are now ready to show that the above observers can secure estimates with arbitrarily small observer errors.

Let estimation error vectors $e_{d_p}(t)$ and $e_{d_\Theta}(t)$ for the position and attitude subsystems be defined as

$$e_{d_p} := \hat{d}_p - d_p \ \ e_{d_\Theta} := \hat{d}_\Theta - d_\Theta \qquad (31)$$

Proposition 1: Under Assumption 1, there exist observer gains $L_j > 0$, $j = p, \Theta$, that are high enough to achieve any prescribed asymptotic estimation precision of the observers (6a) - (6b); i.e. for every $\epsilon > 0$ there exist L_j^*, $j = p, \Theta$, such that for all $L_j \geq L_j^*$ the observer errors satisfy

$$||e_{d_j}(t)||^2 \leq \epsilon, \quad \text{for all} \ t > T^*, \ j = p, \Theta \qquad (32)$$

for a sufficiently large time T^*.

Proof: Note that the position and orientation equations in (4) can be compactly written as:

$$\ddot{p} = G + \frac{U_p}{m} + d_p$$
$$\ddot{\Theta} = \Phi(\Theta, \dot{\Theta}) + U_\Theta \qquad (33)$$

It follows from (6) that

$$\dot{\hat{d}}_p = \dot{z}_p + L_p \ddot{p} = -L_p z_p - L_p[L_p \dot{p} + G + \frac{U_p}{m}]$$
$$+ L_p[G + \frac{U_p}{m} + d_p] = -L_p[z_p + L_p \dot{p}] + L_p d_p$$
$$= -L_p e_{d_p} \qquad (34)$$

It is shown similarly that

$$\dot{\hat{d}}_\Theta = -L_\Theta e_{d_\Theta} \qquad (35)$$

The derivatives of the estimation errors e_{d_j}, $j = p, \Theta$ are hence given by

$$\dot{e}_{d_j} = -L_j e_{d_j} - \dot{d}_j \qquad (36)$$

Since

$$-2e_{d_j}^T \dot{d}_j \leq ||e_{d_j}||^2 + ||\dot{d}_j||^2 \qquad (37)$$

because

$$0 \leq ||e_{d_j} + \dot{d}_j||^2 = e_{d_j}^T e_2 + 2e_{d_j}^T \dot{d}_j + \dot{d}_j^T \dot{d}_j$$
$$= ||e_{d_j}||^2 + ||\dot{d}_j||^2 + 2e_{d_j}^T \dot{d}_j$$

then, defining

$$V_{1j} := e_{d_j}^T e_{d_j} \quad j = p, \Theta \qquad (38)$$

and multiplying (36) by $2\,e_{d_j}^T$ while using (37) together with Assumption 1 yields

$$
\begin{aligned}
\dot{V}_{1j} = 2e_{d_j}^T \dot{e}_{d_j} &= -2e_{d_j}^T L_j e_{d_j} - 2e_{d_j}^T \dot{d}_j \\
&\leq -2e_{d_j}^T L_j e_{d_j} + \|e_{d_j}\|^2 + \|\dot{d}_j\|^2 \\
&\leq -(2L_j + 1)e_{d_j}^T e_{d_j} + D_j^2 \\
&< -(2L_j + 1)V_{1j} + 2D_j^2 \quad j = p, \Theta
\end{aligned}
\tag{39}
$$

Inequality (39) is clearly of the form (7). Hence invoking Lemma 1 basically ends the proof. For complete lucidity, note that in this case, it suffices to pick

$$
L_j^* = \frac{2D_j^2}{\epsilon} - \frac{1}{2}
\tag{40}
$$

to secure that

$$
V_{1j}(t) = \|e_{d_j}\|^2 \leq \epsilon \quad \text{for all} \ \ t \geq T^*; \ j = p, \Theta
\tag{41}
$$

as required. ∎

B. BACKSTEPPING SLIDING MODE CONTROL

This section first describes a regular backstepping technique for the position trajectory tracking control. The backstepping approach is known for its flexibility and capacity to control composite cascade nonlinear systems. With reference to the problem at hand, it will be shown to guarantee stability of translational and rotational subsystems. On the other hand, sliding mode control (SMC) can secure a degree of stability robustness of the closed loop. Such robustness is necessary to compensate for possible model errors and external disturbances so that high-tracking performance can be achieved. A combination of backstepping, SMC, and disturbance estimation performed by the NDO will be proved highly successful in achieving the control goals.

1) POSITION SUBSYTEM CONTROLLER DESIGN

To design the backstepping control for the position subsystem let $p_1 = p$ and $p_2 = \dot{p}$, then the position subsystem in (2a) can be rewritten in a combined form as

$$
\begin{aligned}
\dot{p}_1 &= p_2 \\
\dot{p}_2 &= -ge_3 + \frac{1}{m}U_p + d_p(t)
\end{aligned}
\tag{42}
$$

Defining the position tracking error

$$
e_1 = p_r - p_1
\tag{43}
$$

its time derivative is

$$
\dot{e}_1 = \dot{p}_{1r} - \dot{p}_1 = \dot{p}_{1r} - p_2
\tag{44}
$$

Defining the velocity tracking error as

$$
e_2 = p_{2r} - p_2, \quad p_2 = p_{2r} - e_2
\tag{45}
$$

and substituting (45) into (44) gives

$$
\dot{e}_1 = \dot{p}_{1r} - p_{2r} + e_2
\tag{46}
$$

where p_{2r} is the virtual control law designed to stabilize $\dot{e}_2$

$$
p_{2r} = \dot{p}_{1r} + K_1 e_1, \quad \dot{p}_{2r} = \ddot{p}_{1r} + K_1 \dot{e}_1
\tag{47}
$$

where K_1 is positive definite matrix.

Substituting (47) into (46) yields

$$
\dot{e}_1 = e_2 - K_1 e_1
\tag{48}
$$

Choosing a Lyapunov function candidate as

$$
V_{2p} = \frac{1}{2}e_1^T e_1 + \frac{1}{2}e_2^T e_2
\tag{49}
$$

and taking time derivative of V_{2p}, while using (45) we obtain

$$
\begin{aligned}
\dot{V}_{2p} &= e_1^T \dot{e}_1 + e_2^T \dot{e}_2 \\
&= e_1^T(-K_1 e_1 + e_2) + e_2^T(\ddot{p}_{1r} + K_1 \dot{e}_1 - \dot{p}_2)
\end{aligned}
\tag{50}
$$

Substituting (42) into (50), yields

$$
\begin{aligned}
\dot{V}_{2p} &= -e_1^T k_1 e_1 + e_1^T e_2 + e_2^T(\ddot{p}_{1r} + K_1 \dot{e}_1 \\
&\quad - (-ge_3 + \frac{1}{m}U_p + d_p)) \\
\dot{V}_{2p} &= -e_1^T K_1 e_1 + e_2^T(e_1 + \ddot{p}_{1r} + K_1 \dot{e}_1 \\
&\quad - ge_3 - \frac{1}{m}U_p - d_p)
\end{aligned}
\tag{51}
$$

Now we defined the control input vector as

$$
U_p = m[e_1 + K_1 \dot{e}_1 - ge_3 + \ddot{p}_{1r} - K_2 e_2 - \hat{d}_p]
\tag{52}
$$

where K_2 is another positive definite matrix. The position control law (52) has three components so $U_P = [U_x, U_y, U_z]^T$. Putting $U_p = R(\Theta)U_1 E_3$, the total thrust U_1 is obtained as

$$
U_1 = \frac{U_z}{C_\phi C_\theta}
\tag{53}
$$

and

$$
U_x = \frac{C_\phi s_\theta C_\psi + S_\phi S_\psi}{C_\phi C_\theta}U_1
\tag{54}
$$

$$
U_y = \frac{C_\phi S_\theta S_\psi - S_\phi C_\psi}{C_\phi C_\theta}U_1
\tag{55}
$$

In order to implement the compensation for the disturbance d_p which is needed for improved robustness of the control, the nonlinear disturbance observer (6a) is employed.

Theorem 1: Consider the position error subsystem (43) and (45) in closed loop with the disturbance observer designed as in (6a)-(6b) and the control law designed according to (52) - (53). There exist positive definite gain matrices K_1, K_2 and L_p, such that the closed loop position error satisfies

$$
\|e_1\|^2 + \|e_2\|^2 \leq \epsilon \quad \text{for all} \ \ t \geq T^*
\tag{56}
$$

with any pre-selected precision $\epsilon > 0$ where T^* is sufficiently large.

Proof: Define a Lyapunov function candidate as

$$
V_1 = V_{1p} + V_{2p}
\tag{57}
$$

Considering (52), (53), and taking the time derivative of (57), yields

$$
\begin{aligned}
\dot{V}_1 &= \dot{V}_{1p} + \dot{V}_{2p} \\
&= -e_1^T K_1 e_1 + e_1^T e_2 + e_2^T (\ddot{p}_{1r} + K_1 \dot{e}_1 \\
&\quad - g e_3 + \frac{1}{m} U_p + d_p)) \\
&\quad - e_{d_p}^T (L_p - \frac{1}{2} I_{3x3}) e_{d_p} + \frac{1}{2} D_p^2 \\
&= -e_1^T K_1 e_1 - e_2^T K_2 e_2 + e_2^T (d_p - \hat{d}_p) \\
&\quad - e_{d_p}^T (L_p - \frac{1}{2} I_{3x3}) e_{d_p} + \frac{1}{2} D_p^2 \\
&= -e_1^T K_1 e_1 - e_2^T K_2 e_2 - e_2^T e_{d_p} \\
&\quad - e_{d_p}^T (L_p - \frac{1}{2} I_{3x3}) e_{d_p} + \frac{1}{2} D_p^2 \\
&\leq -e_1^T K_1 e_1 - e_2^T K_2 e_2 - \frac{1}{2} e_2^T e_2 - \frac{1}{2} e_{d_p}^T e_{d_p} \\
&\quad - e_{d_p}^T L_p e_{d_p} + \frac{1}{2} e_{d_p}^T e_{d_p} + \frac{1}{2} D_p^2 \\
&\leq -e_1^T K_1 e_1 - e_2^T (K_2 + \frac{1}{2} I_{3x3}) e_2 \\
&\quad - e_{d_p}^T (L_p - I_{3x3}) e_{d_p} + \frac{1}{2} D_p^2 \\
&< -\delta_1 V_1 + D_p^2
\end{aligned}
\tag{58}
$$

where

$$
\delta_1 = min\{2\lambda_{min}(K_1), 2(\lambda_{min}(K_2) - \frac{1}{2}), 2(\lambda_{min}(L_p - 1))\}
$$

It can be seen that the above gains can be chosen to deliver any magnitude of the tunable coefficient $\delta_1 > 0$. The result of Theorem 1 then follows directly from Lemma 1. ∎

C. ATTITUDE CONTROLLER DESIGN

In this section, the NDO, the backstepping, and sliding control strategies are again combined to deliver attitude control.

In practice, whenever the position of the center of mass of the quadrotor deviates from its reference x_r or y_r the angular position ϕ_r and θ_r also deviate.

The position and attitude control systems are coupled in such a way as to permit the desired attitude angles ϕ_r and θ_r to be tracked by the attitude controller (see Fig. 2) implicitly using the position control law (52). We define the reference trajectory for the attitude subsystem as $\Theta_r = [\phi_r, \theta_r, \psi_r]^T$ where it is assumed that ψ_r is measured directly by a sensor.

The reference angles ϕ_r and θ_r are obtained as follows. Multiplying (54) by $C_\phi C_\theta C_\psi$ and (55) by $C_\phi C_\theta S_\psi$, respectively, yields

$$
U_x C_{\phi_r} C_{\theta_r} C_{\psi_r} = (C_{\phi_r} S_{\theta_r} C_{\psi_r}^2 + S_{\phi_r} S_{\psi_r} C_{\psi_r}) U_1 \tag{59}
$$
$$
U_y C_{\phi_r} C_{\theta_r} S_{\psi_r} = (C_{\phi_r} S_{\theta_r} S_{\psi_r}^2 - S_{\phi_r} S_{\psi_r} C_{\psi_r}) U_1 \tag{60}
$$

Adding (59) to (60) and dividing by $C_\phi C_\theta$ yields,

$$
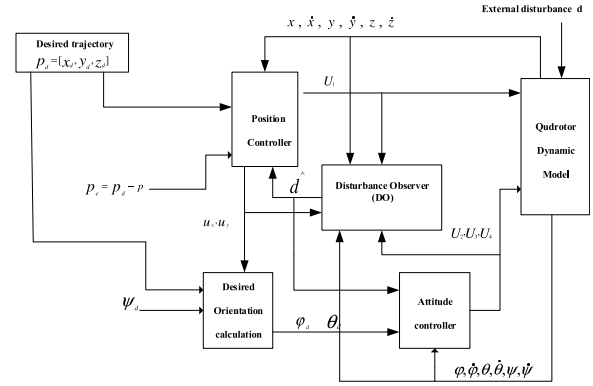U_x C_{\psi_r} + U_y S_{\psi_r} = \tan(\theta_r) U_1 \tag{61}
$$

FIGURE 2. Block diagram of the proposed NDO based backstepping control design.

Then θ_r and ϕ_r are obtained from (59) - (60), and (61) as

$$
\theta_r = \arctan \frac{(U_x C_{\psi_r} + U_y S_{\psi_r})}{U_1} \tag{62}
$$

$$
\phi_r = \arctan \frac{C_{\theta_r}(U_x S_{\psi_r} - U_y C_{\psi_r})}{U_1} \tag{63}
$$

Let $\Theta_1 = \Theta$ and $\Theta_2 = \dot{\Theta}$. Then the rotational subsystem of (2) can be rewritten in a combined form as

$$
\begin{aligned}
\dot{\Theta}_1 &= \Theta_2 \\
\dot{\Theta}_2 &= \Phi(\Theta, \dot{\Theta}) + U_\Theta + d_\Theta(t)
\end{aligned}
\tag{64}
$$

Defining the tracking error

$$
e_3 = \Theta_{1r} - \Theta_1 \tag{65}
$$

its time derivative is written as

$$
\dot{e}_3 = \dot{\Theta}_{1r} - \dot{\Theta}_1 = \dot{x}_{3r} - \Theta_2 \tag{66}
$$

Defining a sliding surface in terms of the error such as:

$$
s = e_4 = \Theta_{2r} - \Theta_2, \quad \Theta_2 = \Theta_{2r} - e_4 \tag{67}
$$

and substituting (67) into (66) gives

$$
\dot{e}_3 = \dot{\Theta}_{1r} - \Theta_{2r} + s \tag{68}
$$

where Θ_{2r} is the virtual control law designed to stabilize $\dot{e}_4$:

$$
\Theta_{2r} = \dot{\Theta}_{1r} + K_3 e_3, \quad \dot{\Theta}_{2r} = \ddot{\Theta}_{1r} - K_3 \dot{e}_3 \tag{69}
$$

where K_3 is a positive definite matrix.

Substituting (69) into (68) yields

$$
\dot{e}_3 = s - K_3 e_3 \tag{70}
$$

Choosing a Lyapunov function candidate as

$$
V_{2\Theta} = \frac{1}{2} e_3^T e_3 + \frac{1}{2} s^T s \tag{71}
$$

and taking time derivative of $V_{2\Theta}$, gives

$$
\begin{aligned}
\dot{V}_{2\Theta} &= e_3^T \dot{e}_3 + s^T \dot{s} \\
&= e_3^T (-K_3 e_3 + s) + s^T (\ddot{\Theta}_{1r} + K_3 \dot{e}_3 - \dot{\Theta}_2)
\end{aligned}
\tag{72}
$$

Substituting (64) into (72), yields

$$
\begin{aligned}
\dot{V}_{2\Theta} &= -e_3^T K_3 e_3 + e_3^T s + s^T (\ddot{\Theta}_{1r} + K_3 \dot{e}_3 \\
&\quad - (\Phi(\Theta, \dot{\Theta}) + U_\Theta) - d_\Theta) \\
&= -e_3^T K_3 e_3 + s^T (e_3 + \ddot{\Theta}_{1r} + K_3 \dot{e}_3 \\
&\quad - \Phi(\Theta, \dot{\Theta}) - U_\Theta - d_\Theta)
\end{aligned}
\tag{73}
$$

Thus the control input vector U_Θ can be defined as

$$
\begin{aligned}
U_\Theta = [e_3 + K_3 \dot{e}_3 - \Phi(\Theta, \dot{\Theta}) + \ddot{\Theta}_{1r} \\
- \hat{d}_\Theta + K_4 s + A \mathrm{sign}(s)]
\end{aligned}
\tag{74}
$$

where K_4 and A are positive definite matrices.

To compensate for d_Θ, the same nonlinear disturbance observer (6b) is used in the attitude system.

The discontinuous function sign(.) in the control law (74) is replaced by a continuous function to reduce the effect of the chattering in the control signal. For instance, the signum function sign(.) can be replaced by the following function [27]

$$
\mathrm{sign}(s) = \frac{s}{\|s\| + \varsigma}
\tag{75}
$$

where ς is a positive tuning parameter that smoothes the discontinuity. It is tuned manually to attenuate the chattering problem.

We prove the following attitude counterpart of Theorem 1.

Theorem 2: Consider the attitude error subsystem (65) and (67) in closed loop with the disturbance observer designed as in (6a)-(6b) and the control law designed according to (74). There exist positive definite gain matrices K_3, K_4, A, and L_Θ, such that the closed loop attitude error satisfies

$$
\|e_3\|^2 + \|e_4\|^2 \le \epsilon \quad \text{for all } t \ge T^*
\tag{76}
$$

with any pre-selected precision $\epsilon > 0$ where T^* is sufficiently large.

Proof: Define a Lyapunov function candidate as:

$$
V_2 = V_{1\Theta} + V_{2\Theta}
\tag{77}
$$

Considering (74), (53), and taking the time derivative of (77), yields

$$
\begin{aligned}
\dot{V}_2 &= \dot{V}_{1\Theta} + \dot{V}_{2\Theta} \\
&= -e_3^T K_3 e_3 + e_3^T s + s^T (\ddot{\Theta}_{1r} + K_3 \dot{e}_3 - \Phi(\Theta, \dot{\Theta}) \\
&\quad + U_\Theta - \hat{d}_\Theta) + e_{d\Theta}^T (L_\Theta - \frac{1}{2} I_{3x3}) e_{d\Theta} + \frac{1}{2} D_\Theta^2 \\
&= -e_3^T K_3 e_3 - s^T K_4 s - s^T e_{d\Theta} - s^T A \, \mathrm{sign}(s) \\
&\quad - e_{d\Theta}^T (L_\Theta - \frac{1}{2} I_{3x3}) e_{d\Theta} + \frac{1}{2} D_\Theta^2 \\
&\le -e_3^T K_3 e_3 - s^T K_4 s - \frac{1}{2} s^T s + \frac{1}{2} e_{d\Theta}^T e_{d1} \\
&\quad - s^T A \, \mathrm{sign}(s) - e_{d\Theta}^T (L_\Theta) e_{d1} \\
&\quad + \frac{1}{2} e_{d\Theta}^T e_{d\Theta} + \frac{1}{2} D_\Theta^2
\end{aligned}
$$

$$
\begin{aligned}
&\le -e_3^T K_3 e_3 - s^T (K_4 + \frac{1}{2} I_{3x3}) s - s^T A \, \mathrm{sign}(s) \\
&\quad - e_{d\Theta}^T (L_\Theta - I_{3x3}) e_{d\Theta} + \frac{1}{2} D_\Theta^2 \\
&\le -e_3^T K_3 e_3 - s^T ((K_4 + A \, \mathrm{sign}(s)) + \frac{1}{2} I_{3x3}) s \\
&\quad - e_{d\Theta}^T (L_\Theta) e_{d\Theta} + \frac{1}{2} D_\Theta^2 \\
&< -\delta_2 V_2 + D_\Theta^2
\end{aligned}
\tag{78}
$$

where

$$
\begin{aligned}
\delta_2 = min\{ & 2\lambda_{min}(K_3), 2(\lambda_{min}(K_4 + A \, \mathrm{sign}(s)) - \frac{1}{2}), \\
& 2(\lambda_{min}(L_\Theta - 1)) \}
\end{aligned}
$$

It can be seen that the above gains can be chosen to deliver any magnitude of the tunable coefficient $\delta_2 > 0$. The result of Theorem 2 then follows directly from Lemma 1. ∎

V. STABILITY ANALYSIS OF THE OVERALL CLOSED LOOP SYSTEM

In view of the results presented in Theorems 1 and 2, it is now straightforward to prove stability for the overall closed loop tracking control system.

Theorem 3: Let the position error subsystem (43) and (45) in closed loop with the disturbance observer designed as in (6a)-(6b) be controlled according to (52) - (53). Also, let the attitude error subsystem (65) and (67) in closed loop with the disturbance observer designed as in (6a)-(6b) be controlled according to (74). Under these conditions, there exists an ensemble of gain matrices K_1, K_2, K_3, K_4, A and L_p, L_Θ such that the overall closed loop control error vector $[e_1, e_2, e_3, e_4]$ is bounded as follows

$$
\|e\|^2 \le \epsilon \quad \text{for all } t \ge T^*
\tag{79}
$$

with any pre-selected precision $\epsilon > 0$ where T^* is sufficiently large.

Proof: Choose the Lyapunov function candidate for the overall closed loop system to be

$$
V = V_1 + V_2
\tag{80}
$$

Differentiating (80) and using (58) and (78) gives

$$
\begin{aligned}
\dot{V} &= \dot{V}_1 + \dot{V}_2 \\
&\le -\delta_1 V_1 + \frac{1}{2} D_2^2 - \delta_2 V_2 + \frac{1}{2} D_1^2 < -\delta V + \gamma
\end{aligned}
\tag{81}
$$

where $\delta = \min\{\delta_1, \delta_2\}$ and $\gamma = \frac{1}{2} D_1^2 + D_2^2$.

Since the coefficients δ_1 and δ_2 are both tunable in their respective position and attitude control subsystems, the δ is also tunable. Hence it again follows from Lemma 1, that for any desired tracking precision $\epsilon > 0$ there exists an ensemble of gain matrices K_1, K_2, K_3, K_4, A, L_p, L_Θ such that the magnitude of both the position and attitude errors do not exceed ϵ on sufficiently long control horizons. ∎

The quadrotor tracking control design is hence complete.

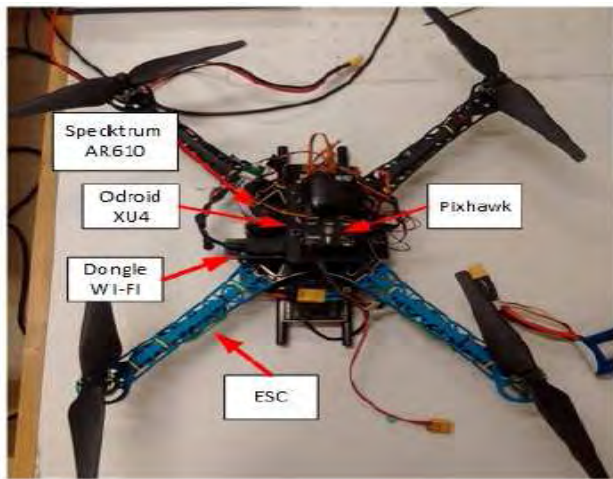## VI. PARAMETER IDENTIFICATION FOR THE QUADROTOR PROTOTYPE

The quadrotor tracking control design described above was tested by way of computer simulations as well as on a real quadrotor system in the Control System Laboratory of École de Technologie Supérieure (ETS), Montreal, Canada.

For the simulation and real flight trajectories to be comparable, the parameters of the real physical system (see (4)) had to be estimated first. To this end we describe the estimation procedure in detail.
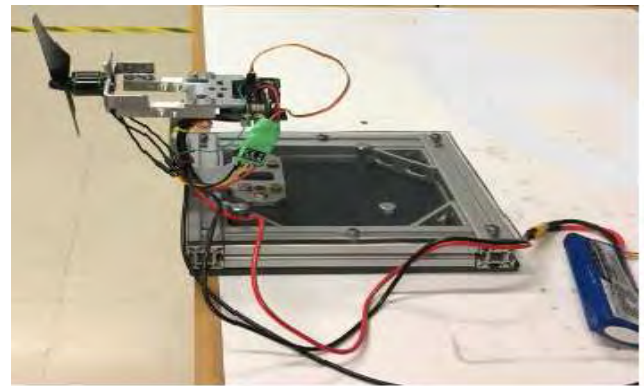
The mass of the quadrotor was simply obtained by weighing the device. However, obtaining the inertia moments was more complex. An RCbenchmark series 1580 dynamometer device was used to determine the relationship between the propellers' speeds and the forces exerted by the motors. A commercial quadrotor, S500 Glass Fiber Quadcopter Frame 480 mm - Integrated PCB was used as the experimental platform (see Figure 3). The measurements necessary for parameter identification were obtained by the use of the solid modeling CAD software (solidworks 2017) (see Fig. 4). Table 1 shows the resulting estimates of the inertia moments for the quadrotor S500.
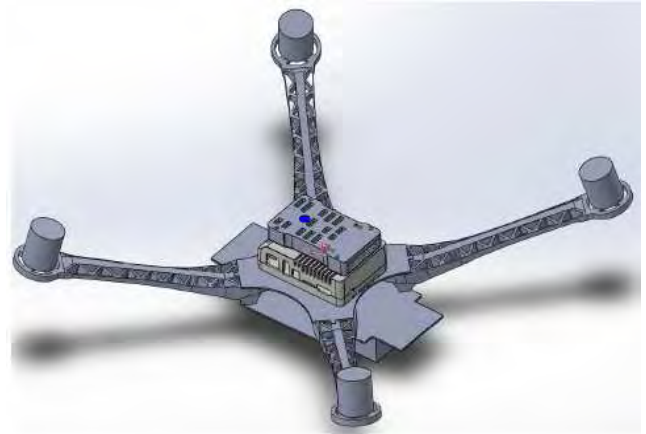
FIGURE 4. Sildworks 3-D model of quadrotor S500.

FIGURE 5. Motor force measuring device.

FIGURE 3. The quadrotor used in real flight tests.

TABLE 1. Inertia moments of quadrotor S500 using Solidworks.

$m(Kg)$	$I_{xx}(Kg \cdot m^2)$	$I_{xx}(Kg \cdot m^2)$	$I_{xx}(Kg \cdot m^2)$
1,354	0.01275	0.01278	0.02271

In practice, the outputs from the designed controller system are the calculated torques corresponding to the measured orientation of the quadrotor and the lift forces. These were then used to determine the forces exerted by each motor. However, the forces control the motors indirectly via PWM signals that regulate the motor speeds. Consequently, in order to find a motors' thrust coefficients, the relationships between the lifting force and the PWM signal for each motor had to be known. The aforementioned device (RCbenchmark Series 1580 Dynamometer, see Fig.5) was again used for

this purpose. This measuring device generates more than four PWM output signals and can measure the speed of a motor. The force exerted by the motor can then be expressed as a function of the pulse width in μs. The obtained measurements are shown in Fig. 6. Using the curve in Fig.6, the relation between the PWM signals and the lift force was approximated by a polynomial in the lift force f_i

$$\text{Pulse Width}(\mu s) = -13.0701f_i^2 + 227.6249f_i + 1036.3 \tag{82}$$

The relation between the torque and the force generated by each motor can be determined using the same device. The motor force and torque measurements are depicted in Fig.7. The curve in Fig.7, was used to determine that the force was approximately a linear function of the torque τ_i.
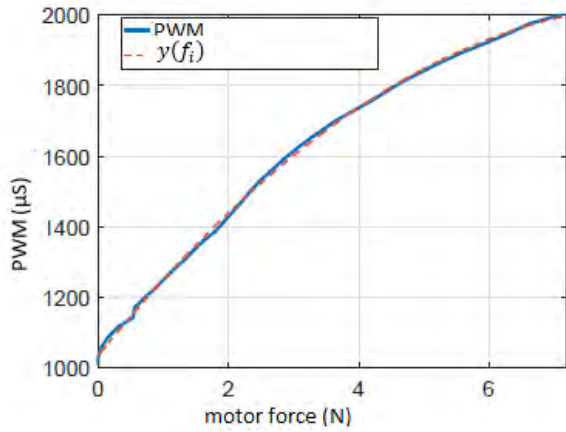
$$f_i = 72.17\tau_i - 0.047 \tag{83}$$

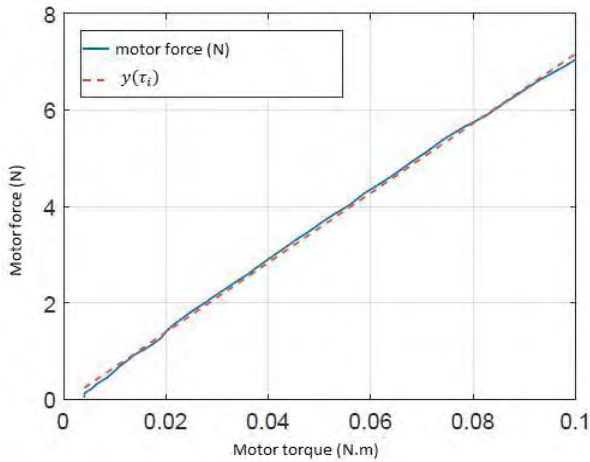**FIGURE 6.** Motor force relative to PWM.

FIGURE 7. The relation between force and torque of the motor.

VII. SIMULATION RESULTS

In order to verify the effectiveness of the proposed method, the simulation results were obtained considering the physical parameters described in the previous section, where the remaining constants were set as follows: $h = 0.225\,m$, $J_R = 3.357 \times 10^{-5} Kgm^2$, and $g = 9.81\,m/s^2$. The quadrotor was required to follow the desired trajectory defined for $t \geq 0$:

$$[x_d, y_d, z_d] = [0.5\sin(2\pi t/40), 0.5\cos(2\pi t/40), 1] \quad (84)$$

Furthermore, the yaw angle reference trajectory was set at $x_{5r} = 0$ rad over the entire simulation horizon. For the purpose of the simulation, the external disturbance vector was considered as a "gust of wind" given by the functions

$$d_1 = [d_x, d_y, d_z]^T$$
$$= [1.5 + 2.5\sin(4t), 1.5 + 2.5\sin(4t), 1.5]N$$
$$d_2 = [d_\phi, d_\theta, d_\psi]^T$$
$$= [2.5\sin(4t), \sin(0.1t), \sin(0.1t)]^T Nm$$

The position and attitude controller gains are 3×3 matrices: $K_1 = \text{diag}[k_x, k_y, k_z]$, $K_2 = \text{diag}[k_{xx}, k_{yy}, k_{zz}]$,

TABLE 2. Controller gains.

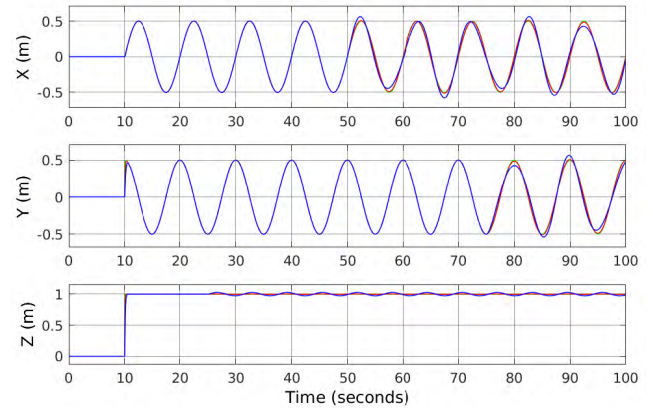| Gain	Value	Gain	Value	Gain	Value
k_x	2.0313	l_y	15	$k_{\psi\psi}$	10.861
k_y	2.0313	l_z	15	l_ϕ	20
k_z	2.216	$k\phi$	12.861	l_ψ	20
k_{xx}	0.0313	k_θ	12.861	l_θ	20
k_{yy}	0.0313	k_ψ	12.861	A_ϕ	0.7
k_{zz}	0.216	$k_{\phi\phi}$	10.861	A_ψ	0.7
l_x	15	$k_{\theta\theta}$	10.861	A_θ	0.7

FIGURE 8. Position tracking in coordinates (x, y, z). graph legend: green - reference trajectory; red - trajectory obtained using the proposed controller; blue - trajectory obtained using the standard backstepping controllers.

$K_3 = \text{diag}[k_\phi, k_\theta, k_\psi]$, $K_4 = \text{diag}[k_{\phi\phi}, k_{\theta\theta}, k_{\psi\psi}]$, and $A = \text{diag}[A_\phi, A_\theta, A_\psi]$. Likewise, the nonlinear observer gains are 3×3 matrices: $L_p = \text{diag}[l_x, l_y, l_z]$ and $L_\Theta = \text{diag}[l_\phi, l_\theta, l_\psi]$. All gains were tuned manually by trial and error in computer simulations. The best values of all gains, which secure the smallest tracking errors, are shown in Table 2.

The simulation results are shown in Fig. 8 - Fig. 13. It can be seen from Fig.8 and Fig. 9 that the quadrotor can track the desired flight path correctly while compensating for the disturbances. Fig.11 also shows good tracking of the attitude reference trajectory. Furthermore, Fig.8 and Fig.11 provide the comparison between the tracking results in position and attitude subsystems obtained using the proposed controller versus the standard backstepping controller. The proposed control-observer scheme is clearly performing better.

The plots of the errors in the position and attitude subsystems are presented in Fig.10 and Fig. 12. It can be seen that the nonlinear disturbance observer can estimate the disturbances quickly and accurately. The control inputs of rotors are presented in Fig. 13.

VIII. EXPERIMENTAL RESULTS

The Pixhawk autopilot was employed as the onboard flight controller to implement the data fusion algorithm and the proposed flight control strategy. For positioning system, a special localization sensor/algorithm (Kinect) is used to capture the position of the quadrotor during the flight. A companion
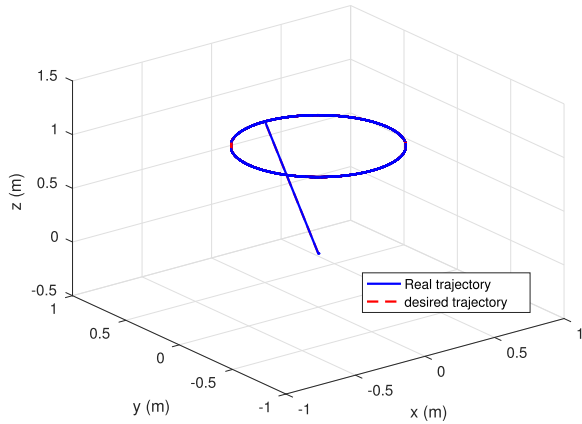
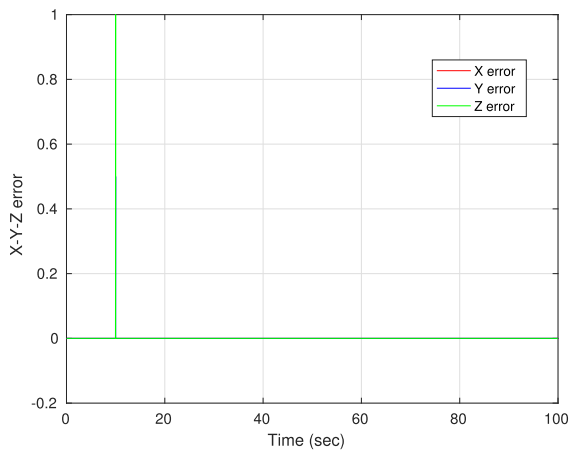**FIGURE 9.** 3D Position tracking in simulation.

FIGURE 10. Position tracking errors in the (x, y, z) coordinates.
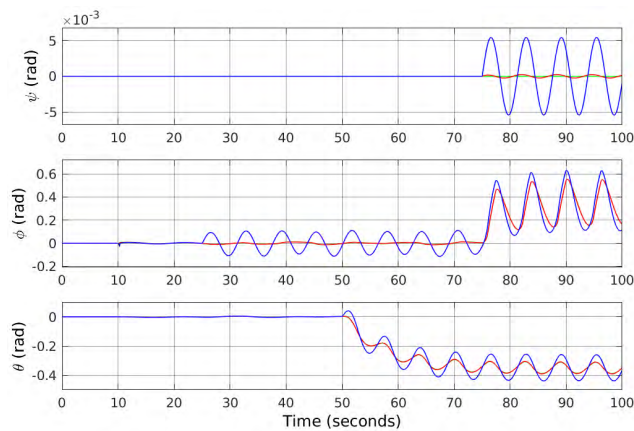

FIGURE 11. Attitude tracking (ϕ, θ, ψ). graph legend: green - reference trajectory; red - trajectory obtained using the proposed controller; blue - trajectory obtained using the standard backstepping controllers.
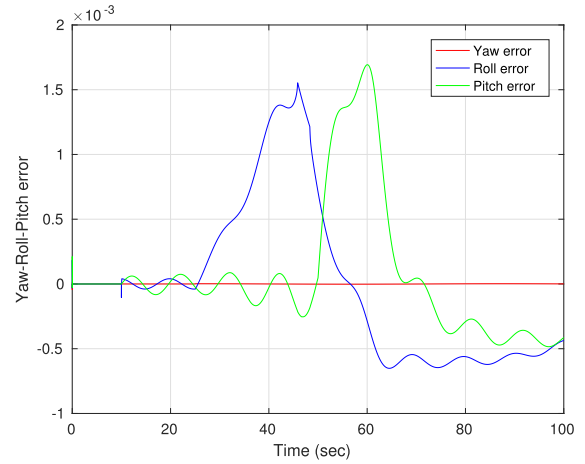

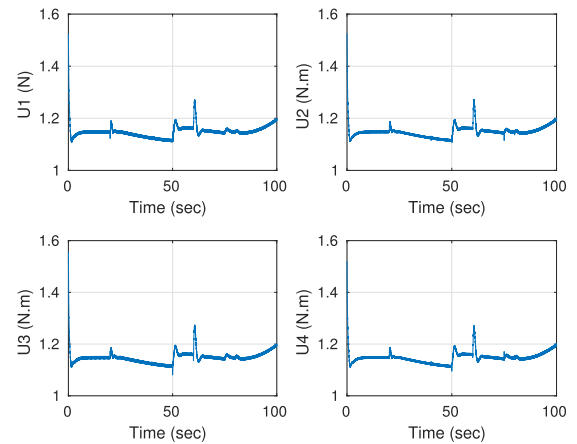**FIGURE 12.** Attitude tracking errors.

**FIGURE 13.** Inputs generated by controllers during simulation.

FIGURE 14. The experimental setup used in real flight tests.

computer (Odroid XU4) is used to interface and communicate with the pixhawk flight controller using the MAVLink protocol over a serial connection. A connection is established for the communication between the companion computer and the ground station. By doing this, the companion computer

gets all the MAVLink data produced by the autopilot and the positioning sensor (Kinect). The controller and estimator parameters employed in the experiment were those listed in Table 2. In practical applications, the attitude gains are
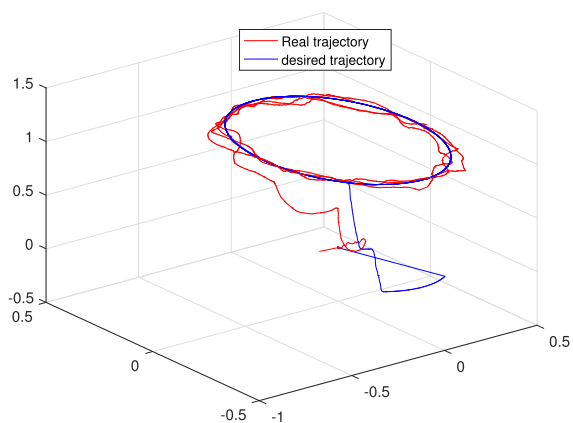
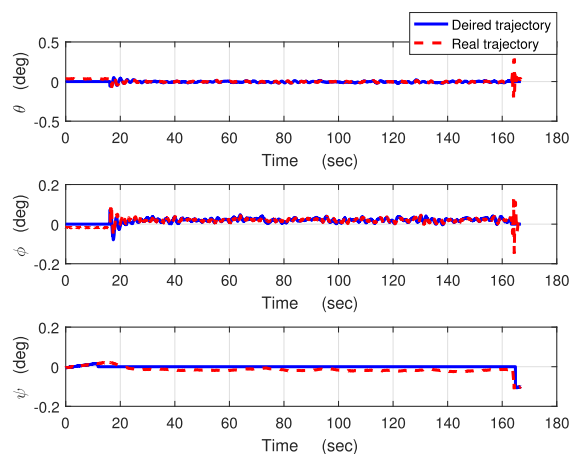**FIGURE 15. Real flight test of 3D position tracking by the proposed controller under the effect of wind gusts.**
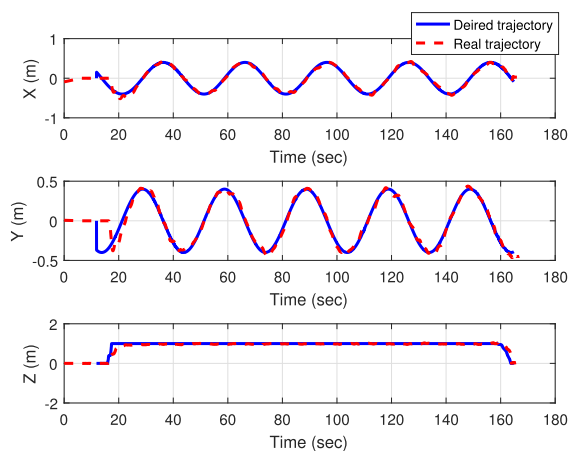
FIGURE 16. Real flight tracking of three position coordinates by proposed controller under the effect of wind gusts. graph legend: red - trajectory obtained using the proposed controller; blue - reference trajectory.
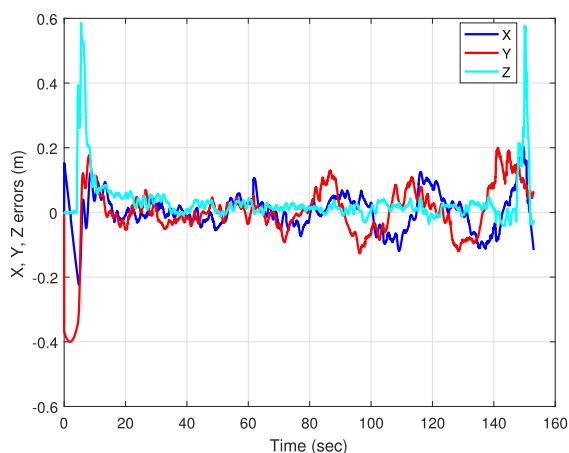
FIGURE 17. The position tracking errors under the effect of wind gusts.

FIGURE 18. Real flight tracking of three attitude angles by proposed controller under the effect of wind gusts. graph legend: red - trajectory obtained using the proposed controller; blue - reference trajectory.
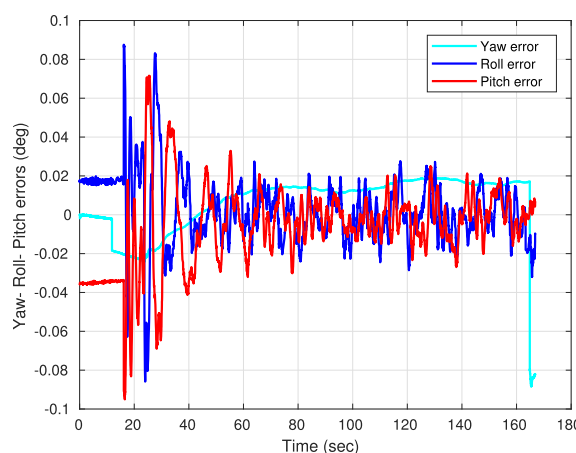

FIGURE 19. The attitude tracking errors under the effect of wind gusts.

The goal of the laboratory experiment was to demonstrate that the designed controller achieves good tracking in the presence of external wind gusts. An electrical fan was used to generate the wind gusts that affect the quadrotor during flight, as shown in Fig. 14. It was required that the quadrotor follows the same trajectory as the one used in computer simulations. The responses of the position and attitude subsystem under wind gusts are depicted in Fig. 15 - Fig. 19 together with the respective tracking errors. The results clearly confirm that the proposed controller is capable of compensating for wind gusts as additional unknown disturbances. The quadrotor tracks the given trajectory with tracking errors that do not exceed 0.2 m.

IX. CONCLUSION

This paper explores a novel approach to robust trajectory tracking control of a quadrotor UAV. A bank of nonlinear disturbance observers is employed in conjunction with a matching set of generalized backstepping and sliding mode controllers to compensate the influence of the unmatched

usually tuned first, followed by the position gains. Based on the permitted overshoot, settling time, the steady-state error requirements, these gains can be tuned by trial and error in hovering conditions.

uncertainties affecting the system during the flight. The stability of the system is guaranteed by designing the backstepping-sliding mode controller combined with the NDO as demonstrated employing a direct Lyapunov analysis. The validity of the developed approach was first confirmed by computer simulations. The performance of the observer-based backstepping-sliding mode control strategy was next extensively validated in real time flight tests using an experimental platform setup. Furthermore, the localization algorithm (Kinect) will be extended to use a precise position measurement from a motion capture system to upgrade the experimental UAV setup. This will enable much better performance of the implemented nonlinear controller.

REFERENCES

[1] N. Fethalla, M. Saad, H. Michalska, and J. Ghommam, "Robust tracking control for a quadrotor UAV," in *Proc. 25th Medit. Conf. Control Automat. (MED)*, Valletta, Malta, Jul. 2017, pp. 1269–1274, doi: 10.1109/MED.2017.7984292.

[2] N. Fethalla, M. Saad, H. Michalska, and J. Ghommam, "Robust observer-based backstepping controller for a quadrotor UAV," in *Proc. IEEE 30th Can. Conf. Elect. Comput. Eng. (CCECE)*, Windsor, ON, Canada, Apr./May 2017, pp. 1–4, doi: 10.1109/CCECE.2017.7946754.

[3] G. M. Hoffmann, H. Huang, S. L. Waslander, and C. J. Tomlin, "Quadrotor helicopter flight dynamics and control: Theory and experiment," in *Proc. AIAA Guid., Navigat., Control Conf. Exhibit*, Hilton Head, SC, USA, Aug. 2007.

[4] E.-H. Zheng, J.-J. Xiong, and J.-L. Luo, "Second order sliding mode control for a quadrotor UAV," *ISA Trans.*, vol. 53, no. 4, pp. 1350–1356, 2014. [Online]. Available: http://www.sciencedirect.com/science/article/pii/S0019057814000512, doi: 10.1016/j.isatra.2014.03.010.

[5] K. Alexis, G. Nikolakopoulos, and A. Tzes, "Model predictive quadrotor control: Attitude, altitude and position experimental studies," *IET Control Theory Appl.*, vol. 6, no. 12, pp. 1812–1827, Aug. 2012, doi: 10.1049/iet-cta.2011.0348.

[6] F. Rinaldi, A. Gargioli, and F. Quagliotti, "PID and LQ regulation of a multirotor attitude: Mathematical modelling, simulations and experimental results," *J. Intell. Robot. Syst.*, vol. 73, nos. 1–4, pp. 33–50, Jan. 2014.

[7] S. Bouabdallah and R. Siegwart, "Backstepping and sliding-mode techniques applied to an indoor micro quadrotor," in *Proc. IEEE Int. Conf. Robot. Automat.*, Barcelona, Spain, 2005, pp. 2247–2252.

[8] C. A. Arellano-Muro, L. F. Luque-Vega, B. Castillo-Toledo, and A. G. Loukianov, "Backstepping control with sliding mode estimation for a hexacopter," in *Proc. 10th Int. Conf. Elect. Eng., Comput. Sci. Autom. Control (CCE)*, Sep./Oct. 2013, pp. 31–36.

[9] T. Madani and A. Benallegue, "Backstepping control for a quadrotor helicopter," in *Proc. IEEE/RSJ Int. Conf. Intell. Robots Syst.*, Beijing, China, Oct. 2006, pp. 3255–3260.

[10] B. Xu, Z. Shi, and C. Yang, "Composite fuzzy control of a class of uncertain nonlinear systems with disturbance observer," *Nonlinear Dyn.*, vol. 80, no. 1, pp. 341–351, 2015.

[11] A. S. Sanca, P. J. Alsina, and J. J. F. Cerqueira, "Stability analysis of a multirotor UAV with robust backstepping controller," in *Proc. Joint Conf. Robot., SBR-LARS Robot. Symp. Robocontrol*, Sao Carlos, Brazil, Oct. 2014, pp. 241–246.

[12] D. Abhijit, L. Frank, and S. Kamesh, "Backstepping approach for controlling a quadrotor using Lagrange form dynamics," *J. Intell. Robot. Syst.*, vol. 56, no. 1, pp. 127–151, Sep. 2009, doi: 10.1007/s10846-009-9331-0.

[13] L. Luque-Vega, B. Castillo-Toledo, and A. G. Loukianov, "Robust block second order sliding mode control for a quadrotor," *J. Franklin Inst.*, vol. 349, no. 2, pp. 719–739, 2012. [Online]. Available: http:www.sciencedirect.com/science/article/pii/S0016003211002882, doi: 10.1016/j.jfranklin.2011.10.017.

[14] T. Madani and A. Benallegue, "Backstepping control with exact 2-sliding mode estimation for a quadrotor unmanned aerial vehicle," in *Proc. IEEE/RSJ Int. Conf. Robots Syst.*, Oct. 2007, pp. 141–146.

[15] J. A. Farrell, M. Polycarpou, M. Sharma, and W. Dong, "Command filtered backstepping," in *Proc. Amer. Control Conf.*, Seattle, WA, USA, Jun. 2008, pp. 1923–1928, doi: 10.1109/ACC.2008.4586773.

[16] J. Yang, S. Li, and X. Yu, "Sliding-mode control for systems with mismatched uncertainties via a disturbance observer," *IEEE Trans. Ind. Electron.*, vol. 60, no. 1, pp. 160–169, Jan. 2013, doi: 10.1109/TIE.2012.2183841.

[17] S. A. Wadoo, "Sliding mode control of crowd dynamics with matched disturbance," in *Proc. IEEE Syst. Conf.*, Montreal, QC, Canada, Apr. 2011, pp. 298–302.

[18] L. Besnard, Y. B. Shtessel, and B. Landrum, "Quadrotor vehicle control via sliding mode controller driven by sliding mode disturbance observer," *J. Franklin Inst.*, vol. 349, no. 2, pp. 658–684, 2012.

[19] X. Yu and O. Kaynak, "Sliding-mode control with soft computing: A survey," *IEEE Trans. Ind. Electron.*, vol. 56, no. 9, pp. 3275–3285, Sep. 2009.

[20] K. Runcharoon and V. Srichatrapimuk, "Sliding mode control of quadrotor," in *Proc. Int. Conf. Technol. Adv. Elect., Electron. Comput. Eng. (TAEECE)*, Konya, Turkey, May 2013, pp. 552–557.

[21] C. T. Ton and W. MacKunis, "Robust attitude tracking control of a quadrotor helicopter in the presence of uncertainty," in *Proc. IEEE 51st IEEE Conf. Decis. Control (CDC)*, Maui, HI, USA, Dec. 2012, pp. 937–942.

[22] A. Polyakov and A. Poznyak, "Invariant ellipsoid method for minimization of unmatched disturbances effects in sliding mode control," *Automatica*, vol. 47, no. 7, pp. 1450–1454, Jul. 2011.

[23] J. M. Andrade-Da Silva, C. Edwards, and S. K. Spurgeon, "Sliding-mode output-feedback control based on LMIs for plants with mismatched uncertainties," *IEEE Trans. Ind. Electron.*, vol. 56, no. 9, pp. 3675–3683, Sep. 2009.

[24] Y. Guo, R. Zhang, and H. Li, "Robust trajectory control for quadrotors with disturbance observer," in *Proc. 35th Chin. Control Conf. (CCC)*, Chengdu, China, Jul. 2016, pp. 10788–10794, doi: 10.1109/ChiCC.2016.7555067.

[25] W.-H. Chen, D. J. Ballance, P. J. Gawthrop, and J. O'Reilly, "A nonlinear disturbance observer for robotic manipulators," *IEEE Trans. Ind. Electron.*, vol. 47, no. 4, pp. 932–938, Aug. 2000.

[26] Y. Wang, D. Zhao, Y. Li, and S. X. Ding, "Unbiased minimum variance fault and state estimation for linear discrete time-varying two-dimensional systems," *IEEE Trans. Autom. Control*, vol. 62, no. 10, pp. 5463–5469, Oct. 2017, doi: 10.1109/TAC.2017.2697210.

[27] M. D. O'Toole, K. Bouazza-Marouf, and D. Kerr, "Chatter suppression in sliding mode control: Strategies and tuning methods," in *ROMANSY 18 Robot Design, Dynamics and Control*, V. Parenti-Castelli and W. Schiehlen, Eds. New York, NY, USA: Springer, 2010.

NURADEEN FETHALLA received the B.S. degree from the Electrical and Computer Engineering Department, Elmergheb University, Alkhoms, Libya, in 2005, and the M.Eng. degree from the Electrical and Computer Engineering Department, Concordia University, Montreal, Canada, in 2012, respectively. He is currently pursuing the Ph.D. degree with the Electronic and Electric Engineering Department, École de technologie supérieure, Montreal. His research interests nonlinear system control and unmanned aerial system control.

MAAROUF SAAD received the bachelor's and master's degrees in electrical engineering from the Ecole Polytechnique of Montreal in 1982 and 1984, respectively, and the Ph.D. degree in electrical engineering from McGill University in 1988. He joined the École de technologie supérieure in 1987, where he is teaching control theory and robotics courses. His research is mainly in nonlinear control and optimization applied to robotics, flight control systems, and multizone power network control.

HANNAH MICHALSKA received the M.Sc. degree in applied mathematics and the Ph.D. degree in control systems from the Imperial College of Science, Technology, and Medicine, London, U.K., in 1989. She was a Post-Doctoral Fellow with the Imperial College Research Centre on Process Systems. In 1992, she took the post of Assistant Professor and then an Associate Professor with the Department of Electrical and Computer Engineering, McGill University, Montreal. Her research interests include control of nonlinear systems, robotics, stabilization, and data fusion.

JAWHAR GHOMMAM received the B.Sc. degree from the Institut Nationale des Sciences Appliques et de Technologies (INSAT), Tunisia, in 2003, the M.Sc. degree in control engineering from the Laboratoire d'Informatique, de Robotique et de Microelectronique, Montpellier, France, in 2004, and the Ph.D. degree in control engineering and industrial computing from the Universit of Orlans, France, in 2008, and the Ecole Nationale d'Ingnieurs de Sfax, Tunisia. He is currently an Assistant Professor of control engineering with INSAT. He is a member of the research unit on Mechatronics and Autonomous systems. His research interests include the nonlinear control of underactuated mechanical systems, adaptive control, guidance and control of underactuated ships, and cooperative motion of nonholonomic vehicles.

● ● ●